

# AN ADAPTIVE MULTILEVEL METHOD FOR TIME-HARMONIC MAXWELL EQUATIONS WITH SINGULARITIES

ZHIMING CHEN\*, LONG WANG<sup>†</sup>, AND WEIYING ZHENG<sup>‡</sup>

**Abstract.** We develop an adaptive edge finite element method based on reliable and efficient residual-based *a posteriori* error estimates for low-frequency time-harmonic Maxwell's equations with singularities. The resulting discrete problem is solved by the multigrid preconditioned minimum residual iteration algorithm. We demonstrate the efficiency and robustness of the proposed method by extensive numerical experiments for cavity problems with singular solutions which includes, in particular, scattering over screens.

**Key words.** Maxwell's equations, singularities of solutions, adaptive finite element method, multigrid method

**AMS subject classifications.** 65N30, 65N55, 78A25

**1. Introduction.** Let  $\Omega \subset \mathbb{R}^3$  be a bounded polygonal domain with two disjoint connected boundaries  $\Gamma$  and  $\Sigma$ . Given a current density  $\mathbf{f}$ , we seek a time-harmonic electric field  $\mathbf{E}$  subject to the perfectly conducting boundary condition on  $\Gamma$  and the impedance boundary condition on  $\Sigma$ :

$$(1.1) \quad \mathbf{curl}(\mu_r^{-1} \mathbf{curl} \mathbf{E}) - \kappa^2 \varepsilon_r \mathbf{E} = \mathbf{f} \quad \text{in } \Omega,$$

$$(1.2) \quad \mu_r^{-1} \mathbf{curl} \mathbf{E} \times \nu - \mathbf{i} \kappa \lambda \mathbf{E}_t = \mathbf{g} \quad \text{on } \Sigma,$$

$$(1.3) \quad \mathbf{E} \times \nu = 0 \quad \text{on } \Gamma,$$

where  $\mathbf{i}$  is the imaginary unit,  $\nu$  is the unit outer normal of the boundary,  $\mathbf{E}_t := (\nu \times \mathbf{E}|_{\Sigma}) \times \nu$ ,  $\varepsilon_r$  is the complex relative dielectric coefficient,  $\mu_r > 0$  is the relative magnetic permeability of the material in  $\Omega$ ,  $\kappa > 0$  is the wave number, and  $\lambda > 0$  is the impedance on  $\Sigma$ . We allow  $\Sigma$  to be empty in which case (1.1) – (1.3) models electromagnetic wave propagation in a cavity with a perfectly conducting wall. For an absorbing boundary condition approximation of a scattering problem,  $\mu_r = \lambda = 1$  on  $\Sigma$  and  $\varepsilon_r = \mu_r = 1$  in a neighborhood of  $\Sigma$ ,  $\mathbf{g}$  can be computed from an incident field  $\mathbf{E}_i$  ( $\mathbf{g} = \mathbf{curl} \mathbf{E}_i \times \nu - \mathbf{i} \kappa \mathbf{E}_{i,t}$ ). In this paper, we focus on low-frequency problems, i.e.  $\kappa$  is not very large.

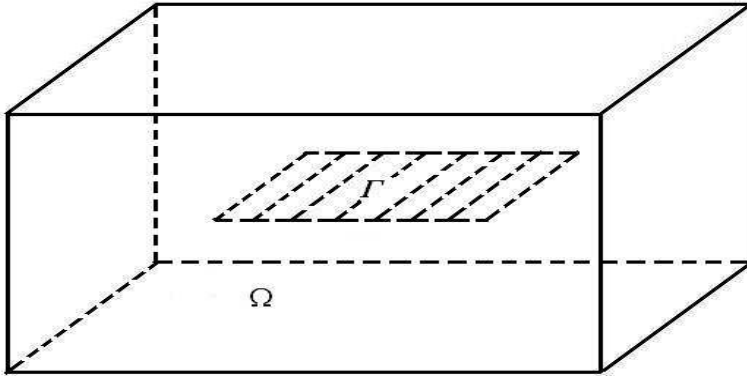
It is now well-known that the solution of the time-harmonic Maxwell equations could have much stronger singularities than the corresponding Dirichlet or Neumann singular functions of the Laplace operator when the computational domain is non-convex or the coefficients of the equations are discontinuous. For example, for the domains that have “screen” or “crack” parts as indicated in Fig 1.1, the regularity of the solution is only in  $\mathbf{H}^s$  with  $s < 1/2$ . In this case the  $\mathbf{H}^1$ -conforming discretization cannot be used directly to solve the time-harmonic cavity problem (1.1)–(1.3). One way to overcome the difficulty is to use the so-called singular field method which

---

\*LSEC, Institute of Computational Mathematics, Academy of Mathematics and System Sciences, Chinese Academy of Sciences, Beijing, 100080, People's Republic of China. This author was supported in part by China NSF under the grant 10025102 and 10428105, and by China MOST under the grant G1999032802 (zmchen@lsec.cc.ac.cn).

<sup>†</sup>LSEC, Institute of Computational Mathematics, Academy of Mathematics and System Sciences, Chinese Academy of Sciences, Beijing, 100080, People's Republic of China (wangl@math.pku.edu.cn).

<sup>‡</sup>LSEC, Institute of Computational Mathematics, Academy of Mathematics and System Sciences, Chinese Academy of Sciences, Beijing, 100080, People's Republic of China. This author was supported in part by China NSF under the grant 10401040 (zwy@lsec.cc.ac.cn).

FIG. 1.1. A domain with screen  $\Gamma$ .

decomposes the solution into a regular part that can be treated by  $\mathbf{H}^1$ -conforming Lagrangian finite elements and an explicit singular part [2], [10], [18], [19]. For the mathematical analysis of the singularities of the solutions of Maxwell equations, we refer to [8], [9], [16], [17], [18], and the references therein.

The first objective of this paper is to explore the possibility of extending the general framework of adaptive finite element methods based on *a posteriori* error estimates initiated in [3] to the time-harmonic Maxwell equations. *A posteriori* error estimates are computable quantities in terms of the discrete solution and known data that measure the actual discrete errors without the knowledge of exact solutions. They are essential in designing algorithms for mesh modification which equi-distribute the computational effort and optimize the computation. The ability of error control and the asymptotically optimal approximation property (see e.g. [11] and [28]) make the adaptive finite element methods attractive for complicated physical and industrial processes (cf. e.g. [12], [14], and [15]).

*A posteriori* error estimates for Nédélec  $\mathbf{H}(\mathbf{curl})$ -conforming edge elements are obtained in [26] for Maxwell scattering problems and in [6] for eddy current problems. The key ingredient in the analysis is the orthogonal Helmholtz decomposition  $\mathbf{v} = \nabla\varphi + \Psi$ , where for any  $\mathbf{v} \in \mathbf{H}(\mathbf{curl}; \Omega)$ ,  $\varphi \in H^1(\Omega)$ , and  $\Psi \in \mathbf{H}(\mathbf{curl}; \Omega)$ . Since a stable edge element interpolation operator is not available for functions in  $\mathbf{H}(\mathbf{curl}; \Omega)$ , some kind of regularity result for  $\Psi \in \mathbf{H}(\mathbf{curl}; \Omega)$  is required. This regularity result is proved in [26] for domains with smooth boundary and in [6] for convex polyhedral domains. The key observation in our analysis is that if one removes the orthogonality requirement in the Helmholtz decomposition, the regularity  $\Psi \in \mathbf{H}^1(\Omega)$  can be proved in the decomposition  $\mathbf{v} = \nabla\varphi + \Psi$  for a large class of non-convex polygonal domains or domains having screens [8], [9], see also [19]. Our extensive numerical experiments for the lowest order edge element indicate that for the cavity problem (1.1)–(1.3) with very strong singularities  $\mathbf{H}^s$  ( $s < 1/2$ ), the adaptive methods based on our *a posteriori* error estimates have the very desirable quasi-optimality property

$$\|\mathbf{E} - \mathbf{E}_k\|_{\mathbf{H}(\mathbf{curl}; \Omega)} \leq C N_k^{-1/3},$$

where  $N_k$  is the number of elements of the  $k$ -th adaptive mesh  $\mathcal{T}_k$ , and  $\mathbf{E}_k$  is the finite element solution over  $\mathcal{T}_k$ .

The second objective of this paper concerns the efficient solution of the large linear system of equations resulting from the edge element discretization of (1.1)–(1.3)

which is in general non-Hermitian and indefinite. We propose to use preconditioned MINRES to solve the linear system of equations with the preconditioner is constructed by the multigrid solver of the stiffness matrix corresponding to the discretization of the following problem

$$(1.4) \quad \mathbf{curl}(\mu_r^{-1} \mathbf{curl} \mathbf{u}) + \kappa^2 |\varepsilon_r| \mathbf{u} = \mathbf{f} \quad \text{in } \Omega,$$

$$(1.5) \quad \mu_r^{-1} \mathbf{curl} \mathbf{u} \times \nu + \kappa \lambda \mathbf{u}_t = \mathbf{g} \quad \text{on } \Sigma,$$

$$(1.6) \quad \mathbf{u} \times \nu = 0 \quad \text{on } \Gamma.$$

Multigrid methods for the edge element discretization of Maxwell's equations have been studied in [1], [22], [23], and the references therein. An important discovery in [23] is that for the  $\mathbf{H}(\mathbf{curl})$ -elliptic problems, multigrid relaxations must be performed both on edges and vertices in order to guarantee the uniform convergence of the multigrid method. We also refer to [5] for the multigrid preconditioned iterative scheme for the Helmholtz equation.

The distinct feature of applying multigrid methods on adaptively refined finite element meshes is that the number of degrees of freedom may not grow exponentially with respect to the number of mesh refinements  $k$ . Following the idea of "local" multigrid in [25] for discrete  $H^1$ -elliptic problems and [7] for discrete  $\mathbf{H}(\mathbf{curl})$ -elliptic problems, at each level  $k$  of our multigrid algorithm for discrete Maxwell problems, we perform Gauß-Seidel relaxations only on new edges, new vertices, and their immediate neighboring edges and vertices (see (4.3) and Algorithm 4.2 below). Our extensive numerical experiments indicate that our multigrid preconditioned MINRES algorithm has the very desirable property: for low-frequency time harmonic Maxwell equations with very strong singularity, the numbers of iterations to reduce the initial residual by a factor  $10^{-8}$  remain nearly fixed on different levels of adaptively refined meshes. We also test the influence of the frequency to the performance of the preconditioner. It indicates that with the frequency of the problem increasing, the number of preconditioned MINRES iterations increases. But for a fixed frequency, it varies very slightly as the number of degrees of freedom increases. We also refer to [33] for the proof of uniform convergence of "local" multigrid method for discrete  $H^1$ -elliptic problems on adaptively refined meshes.

The rest of the paper is organized as follows: In §2, we prove Helmholtz-type decompositions of  $\mathbf{H}(\mathbf{curl}; \Omega)$  and introduce conforming finite element approximations to (1.1)–(1.3). In §3, we derive reliable and efficient residual-based *a posteriori* error estimates. In §4, we describe the preconditioned MINRES algorithm. In §5, we report several numerical experiments to show the competitive performance of the methods proposed in this paper.

## 2. Helmholtz-type decompositions and finite element approximations.

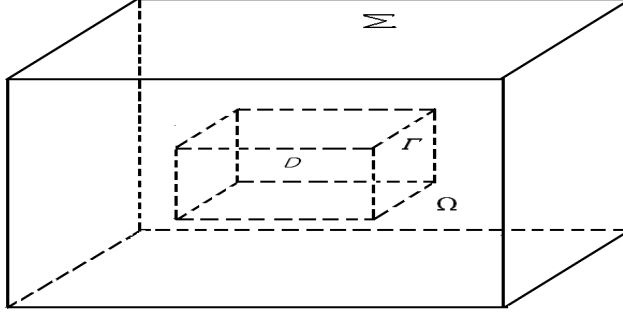
We start by introducing the definition of a "screen".

**DEFINITION 2.1.**  *$F$  is called a Lipschitz screen, if it is a bounded open part of some two-dimensional  $C^2$ -smooth manifold such that its boundary  $\partial F$  is Lipschitz continuous and  $F$  is on one side of  $\partial F$ .*

Let  $\Omega$  be a polyhedral domain in  $\mathbb{R}^3$  which satisfies one of the following assumptions:

**HYPOTHESIS 2.2.**

- (i)  $\Omega$  is a Lipschitz domain and  $\Gamma = \partial D$ , where  $D$  is a bounded Lipschitz domain embedded in the interior of  $\bar{D} \cup \Omega$  (see Fig. 2.1).
- (ii)  $\Gamma$  is a Lipschitz screen such that  $\Omega \cup \Gamma$  is a Lipschitz domain (see Fig. 1.1).

FIG. 2.1. A domain with an inner scatter  $D$ .

(iii)  $\Sigma = \emptyset$  and  $\Gamma = \partial\Omega = \Gamma_{in} \cup \Gamma_{out}$  such that  $\Gamma_{in}$  satisfies the former two assumptions for  $\Gamma$ .

We remark that in each case  $\Omega$  need not to be simply connected and the domain in the second case is even not Lipschitz. In the third case, we actually solve a time-harmonic problem with Dirichlet boundary condition.

We introduce some notation and Sobolev spaces used in this paper.  $L^2(\Omega)$  is the usual Hilbert space of square integrable functions equipped with the following inner product and norm:

$$(u, v) := \int_{\Omega} u(\mathbf{x}) \overline{v(\mathbf{x})} d\mathbf{x} \quad \text{and} \quad \|u\|_{0,\Omega} := (u, u)^{1/2}.$$

$H^m(\Omega) := \{v \in L^2(\Omega) : D^{\xi}v \in L^2(\Omega), |\xi| \leq m\}$  equipped with the following norm and semi-norm

$$\|u\|_{m,\Omega} := \left( \sum_{|\xi| \leq m} \|D^{\xi}u\|_{0,\Omega}^2 \right)^{1/2} \quad \text{and} \quad |u|_{m,\Omega} := \left( \sum_{|\xi|=m} \|D^{\xi}u\|_{0,\Omega}^2 \right)^{1/2},$$

where  $\xi$  represents non-negative triple index.  $H_{\Gamma}^1(\Omega)$  is the subspace of  $H^1(\Omega)$  whose functions have zero traces on  $\Gamma$ . We use boldfaced notations for vectors, such as  $\mathbf{L}^2(\Omega) := (L^2(\Omega))^3$  and so on. The following Sobolev spaces are used in the paper

$$\begin{aligned} \mathbf{H}(\text{div}; \Omega) &:= \{\mathbf{v} \in \mathbf{L}^2(\Omega) : \text{div } \mathbf{v} \in L^2(\Omega)\}, \\ \mathbf{H}(\mathbf{curl}; \Omega) &:= \{\mathbf{v} \in \mathbf{L}^2(\Omega) : \mathbf{curl } \mathbf{v} \in \mathbf{L}^2(\Omega)\}, \\ \mathbf{H}_{\Gamma}(\mathbf{curl}; \Omega) &:= \{\mathbf{v} \in \mathbf{H}(\mathbf{curl}; \Omega) \mid \mathbf{v} \times \boldsymbol{\nu} = 0 \text{ on } \Gamma \text{ and } \mathbf{v}_t \in \mathbf{L}^2(\Sigma)\}. \end{aligned}$$

As usual, we denote  $H_0^1(\Omega) := H_{\partial\Omega}^1(\Omega)$  and  $\mathbf{H}_0(\mathbf{curl}; \Omega) := \mathbf{H}_{\partial\Omega}(\mathbf{curl}; \Omega)$  for  $\Sigma = \emptyset$ .  $\mathbf{H}(\text{div}; \Omega)$ ,  $\mathbf{H}(\mathbf{curl}; \Omega)$ , and  $\mathbf{H}_{\Gamma}(\mathbf{curl}; \Omega)$  are respectively equipped with the following norms:

$$\begin{aligned} \|\mathbf{v}\|_{\mathbf{H}(\text{div}; \Omega)} &:= (\|\mathbf{v}\|_{0,\Omega}^2 + \|\text{div } \mathbf{v}\|_{0,\Omega}^2)^{1/2}, \\ \|\mathbf{v}\|_{\mathbf{H}(\mathbf{curl}; \Omega)} &:= (\|\mathbf{v}\|_{0,\Omega}^2 + \|\mathbf{curl } \mathbf{v}\|_{0,\Omega}^2)^{1/2}, \\ \|\mathbf{v}\|_{\mathbf{H}_{\Gamma}(\mathbf{curl}; \Omega)} &:= (\|\mathbf{v}\|_{0,\Omega}^2 + \|\mathbf{curl } \mathbf{v}\|_{0,\Omega}^2 + \|\mathbf{v}_t\|_{0,\Sigma}^2)^{1/2}. \end{aligned}$$

Let  $\mathbf{f} \in \mathbf{L}^2(\Omega)$  and  $\mathbf{g} \in \mathbf{L}^2(\Sigma)$  satisfying  $\mathbf{g} \cdot \boldsymbol{\nu} = 0$  on  $\Sigma$ . The equivalent weak formulation of (1.1) – (1.3) is: Find  $\mathbf{E} \in \mathbf{H}_\Gamma(\mathbf{curl}; \Omega)$  such that

$$(2.1) \quad a(\mathbf{E}, \mathbf{v}) = \int_\Omega \mathbf{f} \cdot \overline{\boldsymbol{\nabla}} \mathbf{v} + \int_\Sigma \mathbf{g} \cdot \overline{\boldsymbol{\nabla}}_t \mathbf{v} \quad \forall \mathbf{v} \in \mathbf{H}_\Gamma(\mathbf{curl}; \Omega),$$

where

$$(2.2) \quad a(\mathbf{E}, \mathbf{v}) := (\mu_r^{-1} \mathbf{curl} \mathbf{E}, \mathbf{curl} \mathbf{v}) - (\kappa^2 \varepsilon_r \mathbf{E}, \mathbf{v}) - \mathbf{i} \int_\Sigma \kappa \lambda \mathbf{E}_t \cdot \overline{\boldsymbol{\nabla}}_t \mathbf{v}.$$

The existence and uniqueness of the solution of the problem (2.1) under various conditions on the domain  $\Omega$ , the coefficients  $\varepsilon_r$ ,  $\mu_r$  have been studied in [27]. Here for the sake of simplicity we simply assume that the problem (2.1) has a unique solution. Thus there exists a constant  $\beta > 0$  depending only on  $\Omega$ ,  $\varepsilon_r$ ,  $\mu_r$ ,  $\lambda$  and the wave number  $\kappa$  such that [4, Chapter 5]

$$(2.3) \quad \sup_{\mathbf{0} \neq \mathbf{v} \in \mathbf{H}_\Gamma(\mathbf{curl}; \Omega)} \frac{a(\mathbf{E}, \mathbf{v})}{\|\mathbf{v}\|_{\mathbf{H}_\Gamma(\mathbf{curl}; \Omega)}} \geq \beta \|\mathbf{E}\|_{\mathbf{H}_\Gamma(\mathbf{curl}; \Omega)}.$$

Furthermore, it follows from (2.3) that there exists a constant  $C > 0$  independent of  $\mathbf{E}$ ,  $\mathbf{f}$ , and  $\mathbf{g}$  such that

$$(2.4) \quad \|\mathbf{E}\|_{\mathbf{H}_\Gamma(\mathbf{curl}; \Omega)} \leq C(\|\mathbf{f}\|_{0, \Omega} + \|\mathbf{g}\|_{0, \Sigma}).$$

The following Hemholtz-type decomposition theorem is applicable to polyhedral domains with smooth screens  $F$ .

**THEOREM 2.3.** *Let  $\mathcal{D}$  be a bounded domain such that either*

- $\mathcal{D}$  is a Lipschitz domain,

or

- $\mathcal{D}$  has a Lipschitz inner screen  $F$  such that  $\partial \mathcal{D} = \Gamma \cup F$ ,  $\Gamma \cap F = \emptyset$ , and  $\mathcal{D} \cup F$  is a Lipschitz domain (see Fig. 1.1).

Then for any  $\mathbf{v} \in \mathbf{H}_0(\mathbf{curl}; \mathcal{D})$ , there exist  $\psi \in H_0^1(\mathcal{D})$  and  $\mathbf{v}_s \in \mathbf{H}^1(\mathcal{D}) \cap \mathbf{H}_0(\mathbf{curl}; \mathcal{D})$  such that

$$(2.5) \quad \mathbf{v} = \nabla \psi + \mathbf{v}_s \quad \text{in } \mathcal{D},$$

$$(2.6) \quad \|\psi\|_{1, \mathcal{D}} + \|\mathbf{v}_s\|_{1, \mathcal{D}} \leq C \|\mathbf{v}\|_{\mathbf{H}(\mathbf{curl}; \mathcal{D})},$$

where the constant  $C$  depends only on  $\mathcal{D}$ .

*Proof.* The proof for the case when  $\mathcal{D}$  is a Lipschitz domain is contained in [19, Proposition 5.1]. For the completeness we sketch the proof here. The proof below for the case when  $\mathcal{D}$  has a Lipschitz inner screen  $F$  simplifies the argument in [9].

Let  $\mathcal{O} := B(0, R)$  be a ball containing  $\mathcal{D}$ . We extend  $\mathbf{v}$  by zero to the exterior of  $\mathcal{D}$  and denote the extension by  $\tilde{\mathbf{v}}$ . Clearly  $\tilde{\mathbf{v}} \in \mathbf{H}_0(\mathbf{curl}; \mathcal{O})$ . By Theorem 3.4 of [20, p. 45], there exists a  $\mathbf{w} \in \mathbf{H}^1(\mathcal{O})$  such that

$$(2.7) \quad \mathbf{curl} \mathbf{w} = \mathbf{curl} \tilde{\mathbf{v}}, \quad \text{div} \mathbf{w} = 0 \quad \text{in } \mathcal{O},$$

$$(2.8) \quad \|\mathbf{w}\|_{1, \mathcal{O}} \leq C(\|\mathbf{curl} \mathbf{w}\|_{0, \mathcal{O}} + \|\text{div} \mathbf{w}\|_{0, \mathcal{O}}) = C \|\mathbf{curl} \mathbf{v}\|_{0, \mathcal{D}}.$$

Moreover, by (2.7) and Theorem 2.9 of [20, p. 31], there exists a  $\varphi \in H^1(\mathcal{O})/\mathbb{R}$  such that

$$(2.9) \quad \tilde{\mathbf{v}} = \mathbf{w} + \nabla \varphi \quad \text{in } \mathcal{O},$$

$$(2.10) \quad \|\varphi\|_{1, \mathcal{O}} \leq C \|\varphi\|_{1, \mathcal{O}} \leq C \|\mathbf{v}\|_{\mathbf{H}(\mathbf{curl}; \mathcal{D})},$$

$$(2.11) \quad \|\varphi\|_{2, \mathcal{O} \setminus \mathcal{D}} \leq \|\mathbf{w}\|_{1, \mathcal{O}} \leq C \|\mathbf{curl} \mathbf{v}\|_{0, \mathcal{D}}.$$

Since  $\mathcal{O} \setminus \bar{\mathcal{D}}$  is a Lipschitz domain, by the extension theorem [21, Theorem 1.4.3.1, p. 25], there exists an extension of  $\varphi|_{\mathcal{O} \setminus \bar{\mathcal{D}}}$  denoted by  $\tilde{\varphi} \in H^2(\mathbb{R}^3)$  such that

$$(2.12) \quad \tilde{\varphi} = \varphi \quad \text{in } \mathcal{O} \setminus \bar{\mathcal{D}} \quad \text{and} \quad \|\tilde{\varphi}\|_{2, \mathbb{R}^3} \leq C \|\varphi\|_{2, \mathcal{O} \setminus \bar{\mathcal{D}}} \leq C \|\mathbf{v}\|_{\mathbf{H}(\mathbf{curl}; \mathcal{D})}.$$

This completes the proof for the case when  $\mathcal{D}$  is a Lipschitz domain by setting  $\psi = \varphi - \tilde{\varphi} \in H_0^1(\mathcal{D})$  and  $\mathbf{v}_s = \mathbf{w} + \nabla \tilde{\varphi} \in \mathbf{H}^1(\mathcal{D}) \cap \mathbf{H}_0(\mathbf{curl}; \mathcal{D})$ .

If  $\mathcal{D}$  has a Lipschitz screen  $F \subset \mathcal{D}$  such that  $\partial\mathcal{D} = \Gamma \cup F$  and  $\Gamma \cap F = \emptyset$ , we choose a closed  $C^2$ -smooth surface  $F_0 \supset F$  such that  $F_0 \cap \partial\bar{\mathcal{D}} = \emptyset$ . In view of (2.9), we know that  $\nabla_F \varphi = (\nu \times \nabla \varphi) \times \nu = \nu \times (\nu \times \mathbf{w}) \in \mathbf{H}^{1/2}(F)$ , thus  $\varphi|_F \in H^{3/2}(F)$ , where [21, p. 20]

$$H^{m+1/2}(F) = \{v \in L^2(F) : \|v\|_{m+1/2, F} < \infty\}, \quad m = 0, 1,$$

$$\|v\|_{m+1/2, F}^2 = \|v\|_{m, F}^2 + \int_F \int_F \frac{|\nabla_F v(x) - \nabla_F v(y)|^2}{|x - y|^3} ds_x ds_y, \quad m = 0, 1.$$

$H^{3/2}(F_0)$  is defined similarly. Since any function in  $H^{3/2}(D_1)$  can be continuously extended to be a function in  $H^{3/2}(\mathbb{R}^2)$  for any Lipschitz bounded domain  $D_1 \subset \mathbb{R}^2$  [21, Theorem 1.4.3.1, p. 25], we know that  $\varphi|_F$  can be extended continuously to be a function in  $H^{3/2}(F_0)$  by working on the atlas of the  $C^2$ -smooth manifold  $F_0$ . We denote the extension by  $\varphi_F \in H^{3/2}(F_0)$  which satisfies, by (2.8) and (2.11),

$$(2.13) \quad \varphi_F = \varphi \quad \text{on } F,$$

$$(2.14) \quad \|\varphi_F\|_{3/2, F_0} \leq C \|\varphi\|_{3/2, F} \leq C(\|\varphi\|_{1, \mathcal{O}} + \|\mathbf{w}\|_{1, \mathcal{O}}) \leq C \|\mathbf{v}\|_{\mathbf{H}(\mathbf{curl}; \mathcal{D})}.$$

Since  $\tilde{\varphi} \in H^2(\mathbb{R}^3)$ , we have  $\tilde{\varphi} \in H^{3/2}(F_0)$ . Thus  $\varphi_F - \tilde{\varphi} \in H^{3/2}(F_0)$  which we may extend to be a function  $\varphi_0 \in H_0^2(\mathcal{D})$  satisfying

$$(2.15) \quad \varphi_0 = \varphi_F - \tilde{\varphi} \quad \text{on } F \quad \text{and} \quad \|\varphi_0\|_{2, \mathcal{D}} \leq C \|\varphi_F - \tilde{\varphi}\|_{3/2, F_0} \leq C \|\mathbf{v}\|_{\mathbf{H}(\mathbf{curl}; \mathcal{D})},$$

where we have used (2.12)–(2.14). Define  $\psi := \varphi - \tilde{\varphi} - \varphi_0 \in H_0^1(\mathcal{D})$  and  $\mathbf{v}_s := \mathbf{w} + \nabla \tilde{\varphi} + \nabla \varphi_0 \in \mathbf{H}^1(\mathcal{D}) \cap \mathbf{H}_0(\mathbf{curl}; \mathcal{D})$ . Combining (2.8), (2.12), and (2.15) leads to (2.5) and (2.6).  $\square$

**THEOREM 2.4.** *Let  $\Omega$  be a bounded domain with boundary  $\partial\Omega = \Sigma \cup \Gamma$  and satisfy Hypothesis 2.2. For any  $\mathbf{v} \in \mathbf{H}(\mathbf{curl}; \Omega)$  satisfying  $\mathbf{v} \times \nu = 0$  on  $\Gamma$ , there exists a function  $\mathbf{v}_s \in \mathbf{H}^1(\Omega)$  satisfying  $\mathbf{v}_s \times \nu = 0$  on  $\Gamma$  and  $\varphi \in H_1^1(\Omega)$  such that*

$$(2.16) \quad \mathbf{v} = \nabla \varphi + \mathbf{v}_s \quad \text{in } \Omega,$$

$$(2.17) \quad \|\mathbf{v}_s\|_{1, \Omega} + \|\varphi\|_{1, \Omega} \leq C \|\mathbf{v}\|_{\mathbf{H}(\mathbf{curl}; \Omega)}.$$

*Proof.* For the case (iii) in Hypothesis 2.2, Theorem 2.4 follows directly from Theorem 2.3. For the case (i) in Hypothesis 2.2,  $\Gamma = \partial D$  with  $D$  being a bounded Lipschitz domain and  $\bar{D}$  embedded in the interior of  $\Omega \cup \bar{D}$ . Let  $\mathcal{O}$  be a ball containing  $\Omega$ . Extend  $\mathbf{v}$  by zero to  $D$  such that the extension  $\tilde{\mathbf{v}} \in \mathbf{H}(\mathbf{curl}; \Omega \cup \bar{D})$ . By Lemma 2.2 of [13], we may extend  $\tilde{\mathbf{v}}$  to the exterior of  $\Omega \cup \bar{D}$  such that the extension  $E\tilde{\mathbf{v}} \in \mathbf{H}_0(\mathbf{curl}; \mathcal{O})$  and

$$E\tilde{\mathbf{v}} = \tilde{\mathbf{v}} \quad \text{in } \Omega \cup \bar{D},$$

$$\|E\tilde{\mathbf{v}}\|_{\mathbf{H}(\mathbf{curl}; \mathcal{O})} \leq C \|\mathbf{v}\|_{\mathbf{H}(\mathbf{curl}; \Omega)},$$

where  $C$  depends only on  $\Omega$ . Since  $E\tilde{\mathbf{v}} \in \mathbf{H}_0(\mathbf{curl}; \mathcal{O} \setminus \bar{D})$ , by Theorem 2.3, there exist  $\varphi \in H_0^1(\mathcal{O} \setminus \bar{D})$  and  $\mathbf{v}_s \in \mathbf{H}^1(\mathcal{O} \setminus \bar{D}) \cap \mathbf{H}_0(\mathbf{curl}; \mathcal{O} \setminus \bar{D})$  such that

$$\begin{aligned} E\tilde{\mathbf{v}} &= \nabla\varphi + \mathbf{v}_s \quad \text{in } \mathcal{O} \setminus \bar{D}, \\ \|\varphi\|_{1, \mathcal{O} \setminus \bar{D}} + \|\mathbf{v}_s\|_{1, \mathcal{O} \setminus \bar{D}} &\leq C \|E\tilde{\mathbf{v}}\|_{\mathbf{H}(\mathbf{curl}; \mathcal{O} \setminus \bar{D})} \leq C \|\mathbf{v}\|_{\mathbf{H}(\mathbf{curl}; \Omega)}, \end{aligned}$$

where the constant  $C$  depends only on  $\Omega$ . Clearly,  $\varphi$  and  $\mathbf{v}_s$  matches all requirements in Theorem 2.4. The case (ii) of Hypothesis can be proved similarly using Theorem 2.3.  $\square$

REMARK 2.5. *The decompositions in Theorem 2.3 and 2.4 extends the so-called Birman-Solomyak decomposition of  $H_0(\mathbf{curl}; \Omega)$  in [8], [19], and [30].*

Let  $\mathcal{T}_k$  be a sequence of tetrahedral triangulations of  $\Omega$  and  $\mathcal{F}_k$  be the set of faces not lying on  $\Gamma$ ,  $k \geq 0$ . The finite element space  $\mathbf{U}_k$  over  $\mathcal{T}_k$  is defined by

$$\begin{aligned} \mathbf{U}_k := \{ &\mathbf{u} \in \mathbf{H}(\mathbf{curl}; \Omega) : \mathbf{u} \times \boldsymbol{\nu}|_{\Gamma} = \mathbf{0} \quad \text{and} \\ &\mathbf{u}|_T = \mathbf{a}_T + \mathbf{b}_T \times \mathbf{x} \quad \text{with } \mathbf{a}_T, \mathbf{b}_T \in \mathbb{R}^3, \quad \forall T \in \mathcal{T}_k \}. \end{aligned}$$

Degrees of freedom on every  $T \in \mathcal{T}_k$  are  $\int_{E_i} \mathbf{u} \cdot d\mathbf{l}$ ,  $i = 1, \dots, 6$ , where  $E_1, \dots, E_6$  are six edges of  $T$ . For any  $T \in \mathcal{T}_k$  and  $F \in \mathcal{F}_k$ , we denote the diameters of  $T$  and  $F$  by  $h_T$  and  $h_F$  respectively.

The finite element approximation to (2.1) is: Find  $\mathbf{E}_k \in \mathbf{U}_k$  such that

$$(2.18) \quad a(\mathbf{E}_k, \mathbf{v}) = \int_{\Omega} \mathbf{f} \cdot \bar{\nabla} + \int_{\Sigma} \mathbf{g} \cdot \bar{\mathbf{v}}_t, \quad \forall \mathbf{v} \in \mathbf{U}_k.$$

**3. Residual based *a posteriori* error estimates.** Let  $\mathbf{E}$  and  $\mathbf{E}_k$  be the solutions of (2.1) and (2.18) respectively. Define the total error function by  $\mathbf{e}_k := \mathbf{E} - \mathbf{E}_k$ . By (2.3), we know that

$$(3.1) \quad \|\mathbf{e}_k\|_{\mathbf{H}_{\Gamma}(\mathbf{curl}; \Omega)} \leq \beta^{-1} \sup_{\mathbf{v} \in \mathbf{H}_{\Gamma}(\mathbf{curl}; \Omega)} \frac{a(\mathbf{e}_k, \mathbf{v})}{\|\mathbf{v}\|_{\mathbf{H}_{\Gamma}(\mathbf{curl}; \Omega)}}.$$

To derive *a posteriori* error estimates, we introduce the Scott-Zhang Operator  $\mathcal{I}_k : H_{\Gamma}^1(\Omega) \rightarrow V_k$  [32] and the Beck-Hiptmair-Hoppe-Wohlmuth Operator  $\Pi_k : \mathbf{H}^1(\Omega) \cap \mathbf{H}_{\Gamma}(\mathbf{curl}; \Omega) \rightarrow \mathbf{U}_k$  [6], where  $V_k$  is the piecewise linear  $H_{\Gamma}^1$ -conforming finite element space over  $\mathcal{T}_k$  defined by

$$(3.2) \quad V_k := \{v \in H_{\Gamma}^1(\Omega) : v|_T = a_T + \mathbf{b}_T \cdot \mathbf{x} \text{ with } a_T \in \mathbb{R}^1 \text{ and } \mathbf{b}_T \in \mathbb{R}^3, \forall T \in \mathcal{T}_k\}.$$

$\mathcal{I}_k$  and  $\Pi_k$  satisfy the following approximation and stability properties: for any  $T \in \mathcal{T}_k$ ,  $F \in \mathcal{F}_k$ ,

$$(3.3) \quad \begin{cases} \mathcal{I}_k \phi_h = \phi_h & \forall \phi_h \in V_k, \\ \|\nabla \mathcal{I}_k \phi\|_{0, T} & \leq C |\phi|_{1, D_T}, \\ \|\phi - \mathcal{I}_k \phi\|_{0, T} & \leq C h_T |\phi|_{1, D_T}, \\ \|\phi - \mathcal{I}_k \phi\|_{0, F} & \leq C h_F^{1/2} |\phi|_{1, D_F}, \end{cases}$$

and

$$(3.4) \quad \begin{cases} \Pi_k \mathbf{w}_h = \mathbf{w}_h & \forall \mathbf{w}_h \in \mathbf{U}_k, \\ \|\Pi_k \mathbf{w}\|_{\mathbf{H}(\mathbf{curl}; T)} & \leq C \|\mathbf{w}\|_{1, D_T}, \\ \|\mathbf{w} - \Pi_k \mathbf{w}\|_{0, T} & \leq C h_T |\mathbf{w}|_{1, D_T}, \\ \|\mathbf{w} - \Pi_k \mathbf{w}\|_{0, F} & \leq C h_F^{1/2} |\mathbf{w}|_{1, D_F}, \end{cases}$$

where  $D_A$  is the union of elements in  $\mathcal{T}_k$  with non-empty intersection with  $A$ ,  $A = T$  or  $F$ . In (3.3) and (3.4), the constant  $C$  depends on the ratio of the diameter of  $T$  to the diameter of the maximal ball contained in  $T$ . In the procedure of mesh refinements used in ALBERT [31], each element is similar to one of a small number of reference tetrahedra in shape. Thus  $C$  in (3.3)–(3.4) is bounded in the refinement procedure.

By Theorem 2.4, for any  $\mathbf{v} \in \mathbf{H}_\Gamma(\mathbf{curl}; \Omega)$ , there exist a  $\varphi \in H_\Gamma^1(\Omega)$  and a  $\mathbf{v}_s \in \mathbf{H}^1(\Omega) \cap \mathbf{H}_\Gamma(\mathbf{curl}; \Omega)$  such that

$$(3.5) \quad \mathbf{v} = \nabla \varphi + \mathbf{v}_s,$$

$$(3.6) \quad \|\varphi\|_{1,\Omega} + \|\mathbf{v}_s\|_{1,\Omega} \leq C \|\mathbf{v}\|_{\mathbf{H}(\mathbf{curl}; \Omega)},$$

where the constant  $C$  depends only on  $\Omega$ . Since  $\nabla \mathcal{I}_k \varphi$  and  $\Pi_k \mathbf{v}_s$  belong to  $\mathbf{U}_k$ , by the Galerkin orthogonality, we have

$$(3.7) \quad a(\mathbf{e}_k, \mathbf{v}) = a(\mathbf{e}_k, \nabla \varphi - \nabla \mathcal{I}_k \varphi) + a(\mathbf{e}_k, \mathbf{v}_s - \Pi_k \mathbf{v}_s) \quad \forall \mathbf{v} \in \mathbf{H}_\Gamma(\mathbf{curl}; \Omega).$$

For any face  $F \in \mathcal{F}_k$ , assuming  $F = T_1 \cap T_2$ ,  $T_1, T_2 \in \mathcal{T}_k$  and the unit normal  $\nu$  points from  $T_2$  to  $T_1$ , we denote the jump of a function  $v$  across  $F$  by  $[v]_F := v|_{T_1} - v|_{T_2}$ .

LEMMA 3.1. *Let  $\mathbf{g} \in \mathbf{L}^2(\Sigma)$  satisfying  $\operatorname{div}_\Sigma \mathbf{g} \in L^2(\Sigma)$  and  $\mathbf{g} \cdot \nu = 0$  on  $\Sigma$ . There exists a constant  $C_0$  independent of  $\kappa$  and the mesh  $\mathcal{T}_k$  such that*

$$(3.8) \quad a(\mathbf{e}_k, \nabla \varphi - \nabla \mathcal{I}_k \varphi) \leq C_0 \left( \sum_{T \in \mathcal{T}_k} \eta_{0,T}^2 + \sum_{F \in \mathcal{F}_k} \eta_{0,F}^2 + \sum_{F \subset \Sigma} \eta_{0,\Sigma,F}^2 \right)^{1/2} \|\mathbf{v}\|_{\mathbf{H}(\mathbf{curl}; \Omega)},$$

where the the surface divergence  $\operatorname{div}_\Sigma$  on  $\Sigma$  is defined by the  $L^2$ -duality of the surface gradient  $\nabla_\Sigma := -\nu \times (\nu \times \nabla)$ , and the error indicators are defined by

$$\begin{aligned} \eta_{0,T} &:= h_T \|\operatorname{div}(\kappa^2 \varepsilon_r \mathbf{E}_k)\|_{0,T}, \\ \eta_{0,F} &:= h_F^{1/2} \|[\kappa^2 \varepsilon_r \mathbf{E}_k \cdot \nu]_F\|_{0,F}, \\ \eta_{0,\Sigma,F} &:= h_F^{1/2} \|\operatorname{div}_\Sigma(\mathbf{g} + \mathbf{i} \kappa \lambda \mathbf{E}_{k,t})\|_{0,F}. \end{aligned}$$

*Proof.* Since the tangential field  $\mathbf{E}_{k,t}$  is continuous on  $\Sigma$  and piecewise linear,  $\mathbf{E}_{k,t} \in \mathbf{H}(\operatorname{div}_\Sigma; \Sigma)$ . In view that  $\mathbf{f}$  is divergence-free, by (2.1) and the formula of integration by part, we deduce that

$$\begin{aligned} & a(\mathbf{e}_k, \nabla \varphi - \nabla \mathcal{I}_k \varphi) \\ &= (\mathbf{f} + \kappa^2 \varepsilon_r \mathbf{E}_k, \nabla \varphi - \nabla \mathcal{I}_k \varphi) + \int_\Sigma (\mathbf{g} + \mathbf{i} \kappa \lambda \mathbf{E}_{k,t}) \cdot \nabla_\Sigma \overline{(\varphi - \mathcal{I}_k \varphi)} \\ &= - \sum_{T \in \mathcal{T}_k} \int_T \operatorname{div}(\kappa^2 \varepsilon_r \mathbf{E}_k) \overline{(\varphi - \mathcal{I}_k \varphi)} + \sum_{F \in \mathcal{F}_k} \int_F [\kappa^2 \varepsilon_r \mathbf{E}_k \cdot \nu]_F \overline{(\varphi - \mathcal{I}_k \varphi)} \\ & \quad - \sum_{F \subset \Sigma} \int_F \operatorname{div}_\Sigma(\mathbf{g} + \mathbf{i} \kappa \lambda \mathbf{E}_{k,t}) \overline{(\varphi - \mathcal{I}_k \varphi)} \\ &\leq \sum_{T \in \mathcal{T}_k} \|\operatorname{div}(\kappa^2 \varepsilon_r \mathbf{E}_k)\|_{0,T} \|\varphi - \mathcal{I}_k \varphi\|_{0,T} + \sum_{F \in \mathcal{F}_k} \|[\kappa^2 \varepsilon_r \mathbf{E}_k \cdot \nu]_F\|_{0,F} \|\varphi - \mathcal{I}_k \varphi\|_{0,F} \\ & \quad + \sum_{F \subset \Sigma} \|\operatorname{div}_\Sigma(\mathbf{g} + \mathbf{i} \kappa \lambda \mathbf{E}_{k,t})\|_{0,F} \|\varphi - \mathcal{I}_k \varphi\|_{0,F}. \end{aligned}$$

We reach (3.8) by virtue of Schwartz's inequality, (3.3), and (3.6).  $\square$

LEMMA 3.2. *There exists a constant  $C_1$  independent of  $\kappa$  and the mesh  $\mathcal{T}_k$  such that*

$$(3.9) \quad a(\mathbf{e}_k, \mathbf{v}_s - \Pi_k \mathbf{v}_s) \leq C_1 \left( \sum_{T \in \mathcal{T}_k} \eta_{1,T}^2 + \sum_{F \in \mathcal{F}_k} \eta_{1,F}^2 + \sum_{F \subset \Sigma} \eta_{1,\Sigma,F}^2 \right)^{1/2} \|\mathbf{v}\|_{\mathbf{H}(\mathbf{curl}; \Omega)},$$

where

$$\begin{aligned} \eta_{1,T} &= h_T \|\mathbf{f} + \kappa^2 \varepsilon_r \mathbf{E}_k - \mathbf{curl}(\mu_r^{-1} \mathbf{curl} \mathbf{E}_k)\|_{0,T}, \\ \eta_{1,F} &= h_F^{1/2} \|[\mu_r^{-1} \mathbf{curl} \mathbf{E}_k \times \nu]_F\|_{0,F}, \\ \eta_{1,\Sigma,F} &= h_F^{1/2} \|\mathbf{g} + \mathbf{i} \kappa \lambda \mathbf{E}_{k,t} + \nu \times \mu_r^{-1} \mathbf{curl} \mathbf{E}_k\|_{0,F}. \end{aligned}$$

*Proof.* By (2.1) and the formula of integration by part, we deduce that

$$\begin{aligned} & a(\mathbf{e}_k, \mathbf{v}_s - \Pi_k \mathbf{v}_s) \\ &= \sum_{T \in \mathcal{T}_k} \int_T (\mathbf{f} + \kappa^2 \varepsilon_r \mathbf{E}_k - \mathbf{curl} \mu_r^{-1} \mathbf{curl} \mathbf{E}_k) \cdot \overline{(\mathbf{v}_s - \Pi_k \mathbf{v}_s)} \\ & \quad + \sum_{F \in \mathcal{F}_k} \int_F [\nu \times \mu_r^{-1} \mathbf{curl} \mathbf{E}_k]_F \cdot \overline{(\mathbf{v}_s - \Pi_k \mathbf{v}_s)} \\ & \quad + \sum_{F \subset \Sigma} \int_F (\mathbf{g} + \mathbf{i} \kappa \lambda \mathbf{E}_{k,t} + \nu \times \mu_r^{-1} \mathbf{curl} \mathbf{E}_k) \cdot \overline{(\mathbf{v}_s - \Pi_k \mathbf{v}_s)} \\ & \leq \sum_{T \in \mathcal{T}_k} \|\mathbf{f} + \kappa^2 \varepsilon_r \mathbf{E}_k - \mathbf{curl} \mu_r^{-1} \mathbf{curl} \mathbf{E}_k\|_{0,T} \|\mathbf{v}_s - \Pi_k \mathbf{v}_s\|_{0,T} \\ & \quad + \sum_{F \in \mathcal{F}_k} \|[\mu_r^{-1} \mathbf{curl} \mathbf{E}_k \times \nu]_F\|_{0,F} \|\mathbf{v}_s - \Pi_k \mathbf{v}_s\|_{0,F} \\ & \quad + \sum_{F \subset \Sigma} \|\mathbf{g} + \mathbf{i} \kappa \lambda \mathbf{E}_{k,t} + \nu \times \mu_r^{-1} \mathbf{curl} \mathbf{E}_k\|_{0,F} \|\mathbf{v}_s - \Pi_k \mathbf{v}_s\|_{0,F}. \end{aligned}$$

We reach (3.9) by Schwartz's inequality, (3.4), and (3.6).  $\square$

Combining (3.1) and (3.7) – (3.9) leads to the following theorem.

THEOREM 3.3. *Let  $\mathbf{g} \in \mathbf{L}^2(\Sigma)$  satisfying  $\operatorname{div}_\Sigma \mathbf{g} \in L^2(\Sigma)$  and  $\mathbf{g} \cdot \nu = 0$  on  $\Sigma$ . Then*

$$\|\mathbf{e}_k\|_{\mathbf{H}_\Gamma(\mathbf{curl}; \Omega)}^2 \leq \frac{2(C_0^2 + C_1^2)}{\beta^2} \sum_{i=0}^1 \left\{ \sum_{T \in \mathcal{T}_k} \eta_{i,T}^2 + \sum_{F \in \mathcal{F}_k} \eta_{i,F}^2 + \sum_{F \subset \Sigma} \eta_{i,\Sigma,F}^2 \right\},$$

where  $\beta$ ,  $C_0$ , and  $C_1$  is the constants in (2.3), (3.8), and (3.9).

Similar to the argument in [6, Section 5], we can prove the following lower bound estimates.

THEOREM 3.4. *If the material parameters  $\mu_r$ ,  $\varepsilon_r$ , and  $\lambda$  are piecewise constants, there exists a constant  $C$  depending on  $\mu_r$ ,  $\varepsilon_r$ ,  $\lambda$ , and  $\kappa$ , but independent of the mesh*

$\mathcal{T}_k$  such that

$$(3.10) \quad \begin{aligned} & \sum_{T \in \mathcal{T}_k} (\eta_{0,T}^2 + \eta_{1,T}^2) + \sum_{F \in \mathcal{F}_k} (\eta_{0,F}^2 + \eta_{1,F}^2) + \sum_{F \subset \Sigma} (\eta_{0,\Sigma,F}^2 + \eta_{1,\Sigma,F}^2) \\ & \leq C \|\mathbf{e}_k\|_{\mathbf{H}(\mathbf{curl}; \Omega)}^2 + C \sum_{T \in \mathcal{T}_k} h_T^2 \|\mathbf{f} - \mathcal{P}_T \mathbf{f}\|_{0,T}^2 + C \sum_{F \subset \Sigma} h_F \|\operatorname{div}_\Sigma(\mathbf{g} - \mathcal{P}_{\operatorname{div}}^F \mathbf{g})\|_{0,F}^2 \\ & \quad + C \sum_{F \subset \Sigma} h_F \|\mathbf{g} - \mathcal{P}_F \mathbf{g}\|_{0,F}^2, \end{aligned}$$

where  $\mathcal{P}_T: \mathbf{L}^2(T) \rightarrow \mathbf{P}_2(T)$  and  $\mathcal{P}_F: \mathbf{L}^2(F) \rightarrow \mathbf{P}_2(F)$  are  $\mathbf{L}^2$ -projections, and  $\mathcal{P}_{\operatorname{div}}^F: \mathbf{H}(\operatorname{div}_F; F) \rightarrow \mathbf{P}_1(F)$  is the  $\mathbf{H}(\operatorname{div}_F)$ -projection.  $\mathbf{P}_k(D)$  is the space of vector polynomials of maximum degree  $k$  defined on  $D$ ,  $D = T$  or  $F$ .

**4. Multigrid preconditioned MINRES algorithm.** In this section we introduce our preconditioned MINRES (PMINRES) algorithm for solving (2.18). Our preconditioner is a multigrid solver of the stiffness matrix corresponding to the following coercive and Hermitian sesquilinear form on  $\mathbf{U}_k$ :

$$(4.1) \quad a_{mg}(\mathbf{u}, \mathbf{v}) := (\mu_r^{-1} \mathbf{curl} \mathbf{u}, \mathbf{curl} \mathbf{v}) + (\kappa^2 |\varepsilon_r| \mathbf{u}, \mathbf{v}) + \int_\Sigma \kappa \lambda \mathbf{u}_t \cdot \bar{\mathbf{v}}_t.$$

It is easy to see that  $a_{mg}(\cdot, \cdot)$  is the sesquilinear form corresponding to the variational formulation of (1.4)–(1.6).

Let  $\mathcal{T}_0, \dots, \mathcal{T}_J$  be a sequence of nested triangulations by repeated adaptive refinements. Let  $\mathbf{U}_k$  be the finite element space in (2.18) and  $V_k$  be the linear Lagrangian finite element space in (3.2) over  $\mathcal{T}_k$ . Denote the canonical basis of  $\mathbf{U}_k$  by  $\{\mathbf{w}_1^{(k)}, \dots, \mathbf{w}_{n_k}^{(k)}\}$  and the canonical basis of  $V_k$  by  $\{\phi_1^{(k)}, \dots, \phi_{\bar{n}_k}^{(k)}\}$ , where  $n_k$  and  $\bar{n}_k$  are respectively the numbers of edges and vertices not on  $\Gamma$ .

We now specify the local multigrid algorithm for the solution of the following algebraic system of equations

$$(4.2) \quad A_k X_k = F_k,$$

where  $A_k = \left( a_{mg}(\mathbf{w}_i^{(k)}, \mathbf{w}_j^{(k)}) \right)_{n_k \times n_k}$ . The algorithm is based on the following space decomposition proposed in [7]:

$$(4.3) \quad \mathbf{U}_J = \mathbf{U}_0 + \sum_{k=1}^J \sum_{E \in \mathcal{E}_k^{\text{new}}} \operatorname{span}\{\mathbf{w}_E\} + \sum_{k=1}^J \sum_{a \in \mathcal{V}_k^{\text{new}}} \operatorname{span}\{\nabla \phi_a\},$$

where  $\mathcal{E}_k^{\text{new}}$  and  $\mathcal{V}_k^{\text{new}}$  are respectively the set of edges and the set of vertices in new elements of  $\mathcal{T}_k$ . None of the edges and vertices in (4.3) is on  $\Gamma$ . The algorithm of multigrid V-cycle is defined recursively as follows:

ALGORITHM 4.1. Multigrid V-cycle:

MGsolver( $A_J, F_J, m$ )

{

  Given initial guess  $\mathcal{X}_0$

  For  $l = 0 : m - 1$

$\mathcal{X}_{l+1} \leftarrow \text{MG}(J, A_J, F_J, \mathcal{X}_l)$

}

```

    return  $\mathcal{X}_m$ 
}
MG( $j, A_j, f, x$ ),  $j = 0, \dots, J$  recursively defined by
{
  if ( $j = 0$ )
    return  $A_0^{-1}f$ 
  else
    {
       $x \leftarrow \text{GSsmooth}(A_j, f, x)$  [Pre-smoothing]
       $y \leftarrow \text{MG}(j-1, A_{j-1}, \mathcal{R}_j^{j-1}(f - A_j x), 0)$ 
       $x \leftarrow x + \mathcal{I}_{j-1}^j y$ 
       $x \leftarrow \text{GSsmooth}(A_j, f, x)$  [Post-smoothing]
    }
}

```

In Algorithm 4.1,  $\mathcal{I}_{j-1}^j$  is a  $n_j \times n_{j-1}$  matrix reflecting the identical embedding  $\mathbf{U}_{j-1} \hookrightarrow \mathbf{U}_j$  such that

$$\sum_{i=1}^{n_{j-1}} y_i \mathbf{w}_i^{(j-1)} = \sum_{i=1}^{n_j} \left( \mathcal{I}_{j-1}^j y \right)_i \mathbf{w}_i^{(j)}.$$

We choose the restriction matrix  $\mathcal{R}_j^{j-1}$  to be the transpose of  $\mathcal{I}_{j-1}^j$ , that is  $\mathcal{R}_j^{j-1} = \left( \mathcal{I}_{j-1}^j \right)^T$ . Define  $A_{j,\nabla} = \left( a_{mg}(\nabla \phi_m^{(j)}, \nabla \phi_n^{(j)}) \right)_{\bar{n}_j \times \bar{n}_j}$  and  $\mathcal{I}_V^E$  to be a  $n_j \times \bar{n}_j$  matrix reflecting the identical embedding  $\nabla V_j \hookrightarrow \mathbf{U}_j$  such that

$$\sum_{i=1}^{\bar{n}_j} y_i \nabla \phi_i^{(j)} = \sum_{i=1}^{n_j} (\mathcal{I}_V^E y)_i \mathbf{w}_i^{(j)}.$$

$\text{GSsmooth}(A_j, f, x)$  is the Gauß-Seidel iterations on level  $j$  with initial guess  $x$ .

ALGORITHM 4.2. Gauß-Seidel sweeping:

```

GSsmooth( $A_j, f, x$ )
{
  Gauß-Seidel sweep on d.o.f.s of  $A_j x = f$  related to  $\mathcal{E}_j^{\text{new}}$ 
   $y \leftarrow f - A_j x$ 
   $y_\nabla \leftarrow (\mathcal{I}_V^E)^T y$ 
   $x_\nabla \leftarrow 0$ 
  Gauß-Seidel sweep on d.o.f.s of  $A_{j,\nabla} x_\nabla = y_\nabla$  related to  $\mathcal{V}_j^{\text{new}}$ 
  return  $x + \mathcal{I}_V^E x_\nabla$ 
}

```

**5. Adaptive algorithm and numerical results.** The implementation of our adaptive algorithm is based on the adaptive finite element package ALBERT [31] and is carried out on Origin 3800. We define the local *a posteriori* error estimator over an element  $T \in \mathcal{T}_h$  by

$$\eta_T := \left\{ \eta_{0,T}^2 + \eta_{1,T}^2 + \frac{1}{2} \sum_{F \subset \partial T} (\eta_{0,F}^2 + \eta_{1,F}^2 + \eta_{0,\Sigma,F}^2 + \eta_{1,\Sigma,F}^2) \right\}^{1/2}$$

and define the global *a posteriori* error estimate, the maximal element error estimate over  $\mathcal{T}_h$  respectively by

$$(5.1) \quad \eta_h := \left( \sum_{T \in \mathcal{T}_h} \eta_T^2 \right)^{1/2}, \quad \eta_{\max} = \max_{T \in \mathcal{T}_h} \eta_T.$$

Now we describe the adaptive algorithm used in this paper.

ALGORITHM 5.1. Given a tolerance  $Tol > 0$  and the initial mesh  $\mathcal{T}_0$ . Set  $\mathcal{T}_h = \mathcal{T}_0$ .

- (I) Solve the discrete problem (2.18) on  $\mathcal{T}_0$ .
- (II) Compute the local error estimator  $\eta_T$  on each  $T \in \mathcal{T}_0$ , the global error estimate  $\eta_h$ , and the maximal element error estimate  $\eta_{\max}$ .
- (III) While  $\eta_h > Tol$  do
  - Refine the mesh  $\mathcal{T}_h$  according to the following strategy

if  $\eta_T > \frac{3}{5}\eta_{\max}$ , refine the element  $T \in \mathcal{T}_h$ .

- Solve the discrete problem (2.18) on  $\mathcal{T}_h$ .
- Compute the local error estimator  $\eta_T$  on each  $T \in \mathcal{T}_h$ , the global error estimate  $\eta_h$ , and the maximal element error estimate  $\eta_{\max}$ .

end while.

In the following, we report several numerical experiments to demonstrate the competitive behavior of the proposed algorithm. In our PMINRES solver, we use only one step of local multigrid iteration and one Gauß-Seidel sweep for pre- and post-smoothing.

EXAMPLE 5.1. We consider the Maxwell equation (1.1) on the three-dimensional “L-shaped” domain  $\Omega = (-1, 1)^3 \setminus \{(0, 1) \times (-1, 0) \times (-1, 1)\}$ . Let  $\mu_r = \kappa = \varepsilon_r = 1$  and  $\Gamma = \partial\Omega$ . The non-dimensional wavelength is  $2\pi/(\kappa \text{diam}(\Omega)) = \pi/\sqrt{3}$ , since the diameter of  $\Omega$  is  $2\sqrt{3}$ . The Dirichlet boundary condition and the source  $\mathbf{f}$  are so chosen that the exact solution is  $\mathbf{E} := \nabla \{r^{1/2} \sin(\phi/2)\}$  in cylindrical coordinates.

Fig. 5.1 shows the curves of  $\log \|\mathbf{E} - \mathbf{E}_k\|_{\mathbf{H}(\text{curl}; \Omega)}$  versus  $\log N_k$ , where  $N_k$  is the number of elements and  $\mathbf{E}_k$  is the finite element solution of (2.18) over the mesh  $\mathcal{T}_k$ . Fig. 5.2 shows the  $\log \eta_k - \log N_k$  curves, where  $\eta_k$  is the associated *a posteriori* error estimate over  $\mathcal{T}_k$  defined in Theorem 3.3. They indicate that the adaptive meshes and the associated numerical complexity are quasi-optimal, i.e.

$$(5.2) \quad \eta_k = C N_k^{-1/3} \quad \text{and}$$

$$(5.3) \quad \|\mathbf{E} - \mathbf{E}_k\|_{\mathbf{H}(\text{curl}; \Omega)} = C N_k^{-1/3}$$

are valid asymptotically. They also show clearly the advantage of adaptive method compared with the uniform refinements.

Table 5.1 shows the numbers of PMINRES iterations required to reduce the initial residual by a factor  $10^{-8}$  on different levels. We observe that PMINRES algorithm converges in very few steps with the number of degrees of freedom varying from 722 to 1,616,983. Fig. 5.3 shows the CPU time versus the number of degrees of freedom on different adaptive meshes.

Fig. 5.4 shows an adaptive mesh of 18,874,368 elements after 12 adaptive iterations. We observe that the mesh is locally refined near the corner line  $x_1 = x_2 = 0$  where the solution is singular.

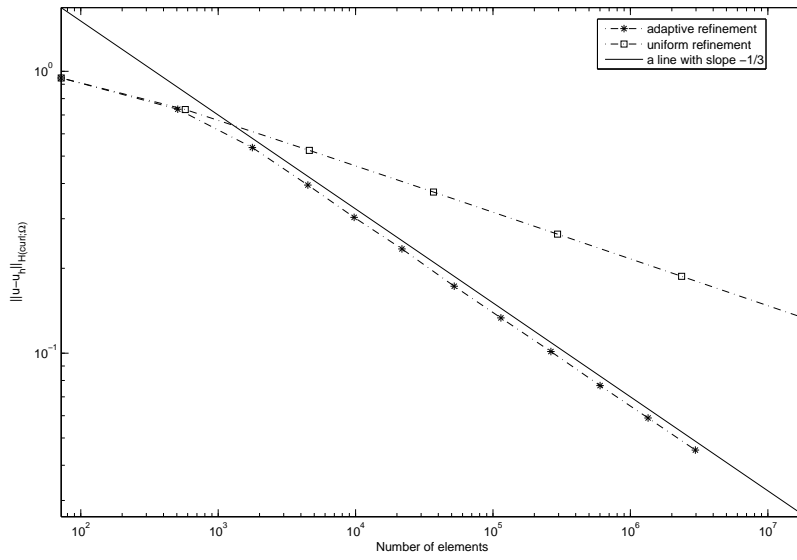


FIG. 5.1. Quasi-optimality of the adaptive mesh refinements of the error  $\|u - u_h\|_{\mathbf{H}(\text{curl}; \Omega)}$  (Example 5.1).

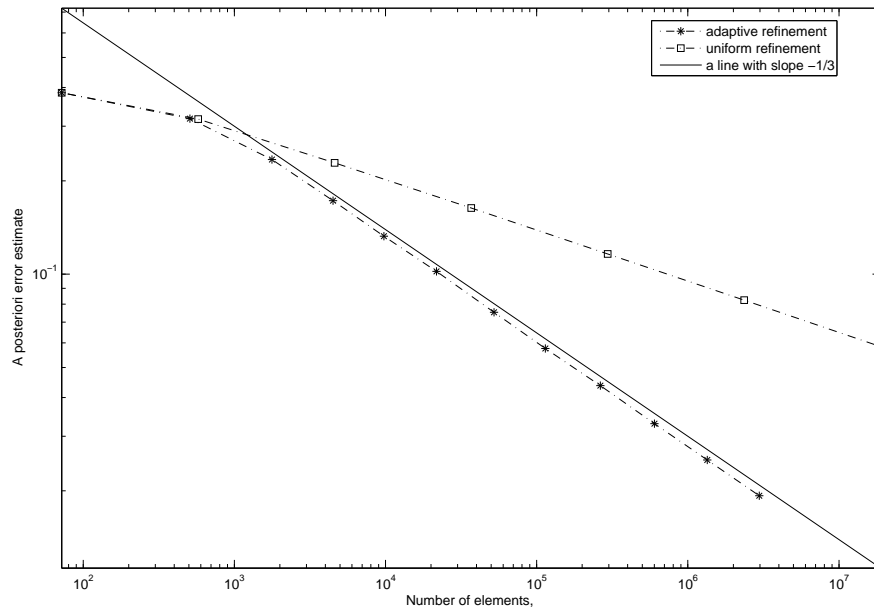


FIG. 5.2. Quasi-optimality of the adaptive mesh refinements of the a posteriori error estimate (Example 5.1).

TABLE 5.1

The Number of *PMINRES* iterations ( $N_{itrs}$ ) required to reduce the initial residual by a factor  $10^{-8}$  (Example 5.1) .

Level	1	3	5	7	8	9	10
DOFs	722	5668	26810	138667	319360	725217	1616983
$N_{itrs}$	5	6	6	7	7	8	8

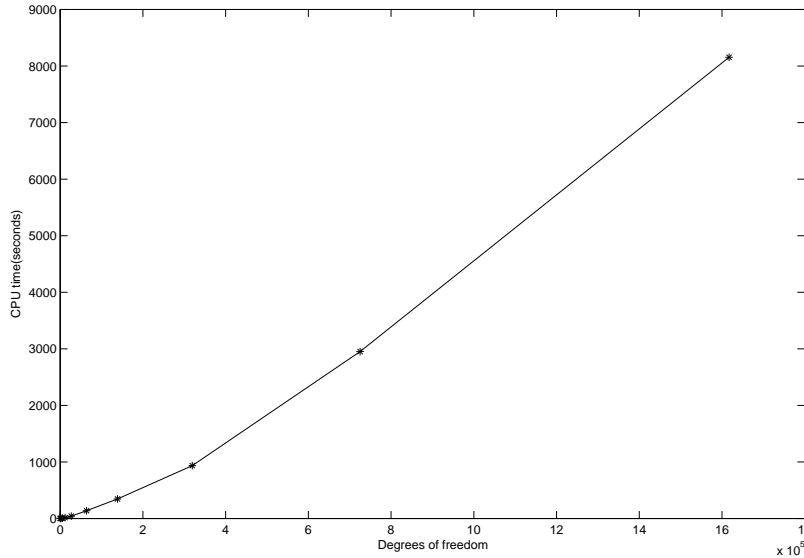


FIG. 5.3. CPU time for *PMINRES* iterations on adaptively refined grids (Example 5.1).

EXAMPLE 5.2. We consider a time-harmonic problem containing an inner screen  $\Gamma := \{(x, y, z) : -0.5 \leq x, z \leq 0.5, y = 0\}$ . We define  $\Omega = (-1, 1)^3 \setminus \Gamma$  and  $\Sigma = \partial\Omega \setminus \Gamma$ . We set  $\mu_r = \varepsilon_r = \lambda = 1$  in (1.1) and (1.2) and define

$$\mathbf{f} := \mathbf{0}, \quad \mathbf{g} := \mathbf{curl} \mathbf{E}_i \times \boldsymbol{\nu} - \mathbf{i} \kappa \mathbf{E}_{i,t},$$

where  $\mathbf{E}_i = (e^{iy}, 0, e^{iy})^T / \sqrt{2}$  perpendicular to the perfect conducting “screen”. Thus (1.1)–(1.3) models the scattering by  $\Gamma$  under the incident field  $\mathbf{E}_i$ . In this case, only  $\mathbf{H}^s$ -regularity ( $s < 1/2$ ) of the solution is guaranteed.

In this experiment, we test the performance of the a posteriori error estimate and the preconditioned MINRRS algorithm under different frequencies, i.e.  $\kappa^2 = 1, 1.5, 10, 20, 36, 64, 100$  in (1.1) and (1.2). The non-dimensional wavelength here is  $\pi/(\sqrt{3}\kappa)$ . Fig. 5.5 – Fig. 5.7 show the results for  $\kappa = 1$ , while Fig. 5.8 and Fig. 5.9 show the result for  $\kappa > 1$ .

Fig. 5.5 shows the  $\log \eta_k - \log N_k$  curves and indicates that the adaptive meshes and the associated numerical complexity are quasi-optimal and (5.2) is valid asymptotically. It also shows clearly the advantage of adaptive method compared with the uniform refinements.

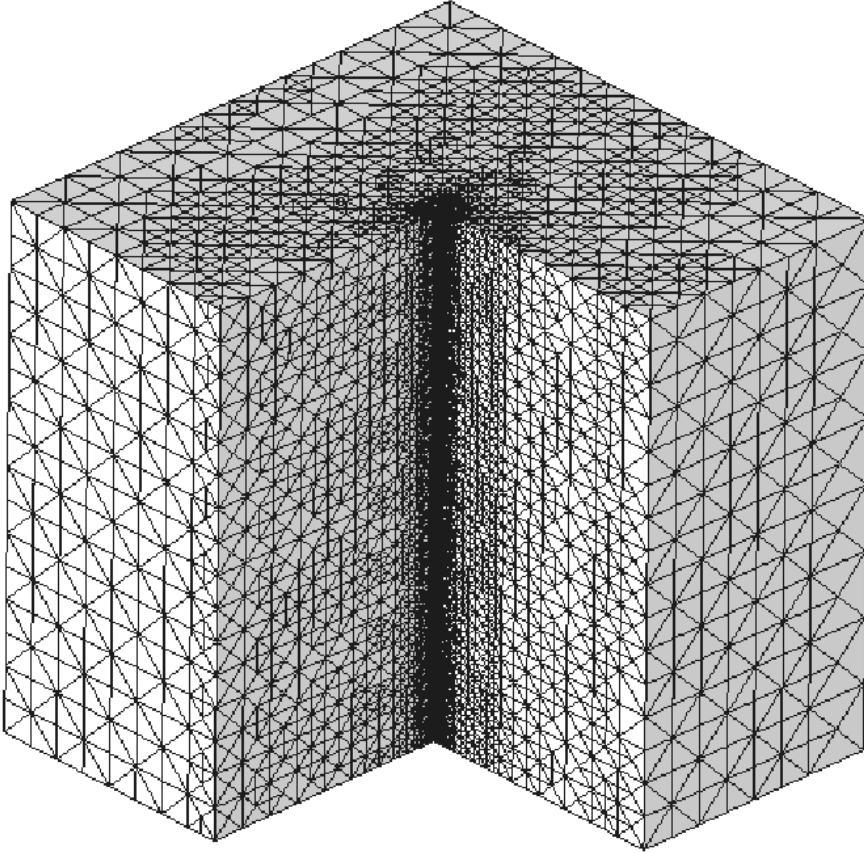


FIG. 5.4. An adaptively refined mesh of 18,874,368 elements after 12 adaptive iterations (Example 5.1).

Fig. 5.6 shows the CPU time versus the number of degrees of freedom on different adaptive meshes.

Fig. 5.7 shows an adaptive mesh of 2,947,848 elements after 11 adaptive iterations. We observe that the mesh is locally refined near the boundary of the “screen”.

Fig. 5.8 shows the  $\log \eta_k - \log N_k$  curves for  $\kappa^2 = 1.5, 10, 20, 36, 64, 100$ . It indicates that the adaptive meshes and the associated numerical complexity are quasi-optimal and (5.2) is valid asymptotically for all these values of  $\kappa$ .

Fig. 5.9 shows the CPU time versus the number of degrees of freedom on different adaptive meshes for  $\kappa^2 = 1.5, 10, 20, 36, 64, 100$ . All lines show a quasi-linear increasing of the CPU time of the solution of the algebraic system with respect to the number of degrees of freedom. However, when  $\kappa^2 \geq 20$ , the CPU time increases dramatically compared with the time for small  $\kappa$ .

Table 5.2 shows the numbers of PMINRES iterations required to reduce the initial residual by a factor  $10^{-8}$  for  $\kappa^2 = 1, 1.5, 10, 20, 36, 64, 100$  on different levels. We observe that it remains nearly fixed for  $\kappa^2 \leq 10$  with the number of degrees of freedom varying from 1,322 to 1,513,049. When  $\kappa^2 \geq 20$ , the number of iterations increases

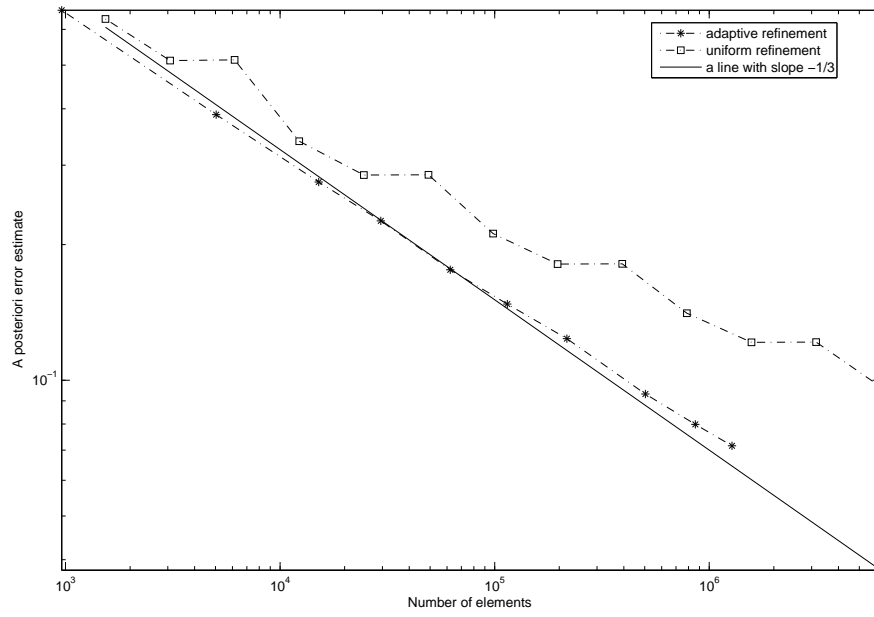


FIG. 5.5. *Quasi-optimality of the adaptive mesh refinements of the a posteriori error estimate (Example 5.2).*

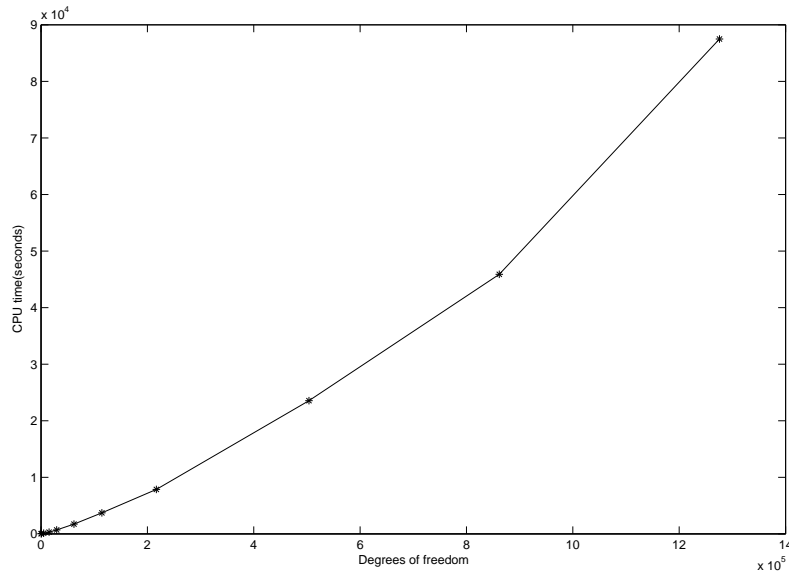


FIG. 5.6. *CPU time for PMINRES iterations on adaptively refined meshes (Example 5.2).*

rapidly as  $\kappa$  increases, but it varies slightly for all  $\kappa$  with the number of degrees of freedom increasing.

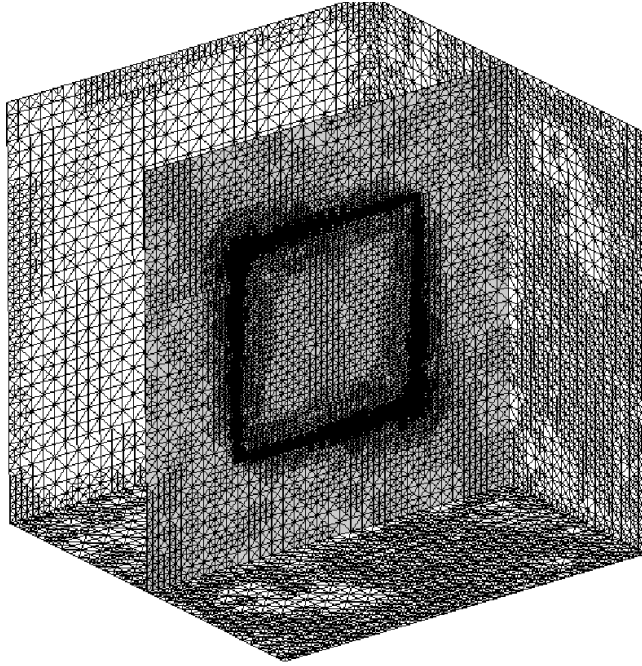


FIG. 5.7. An adaptively refined mesh of 2,947,848 elements after 11 adaptive iterations (Example 5.2).

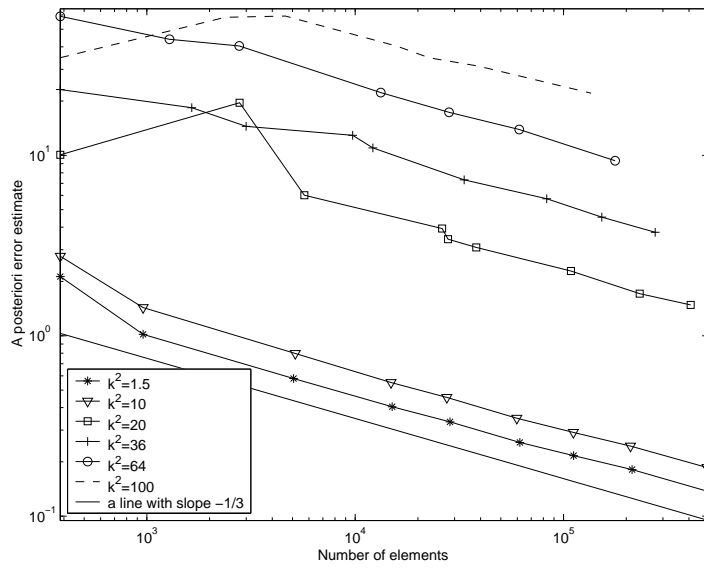


FIG. 5.8. Quasi-optimality of the adaptive mesh refinements of the a posteriori error estimate for  $\kappa^2 = 1.5, 10, 20, 36, 64, 100$  (Example 5.2).

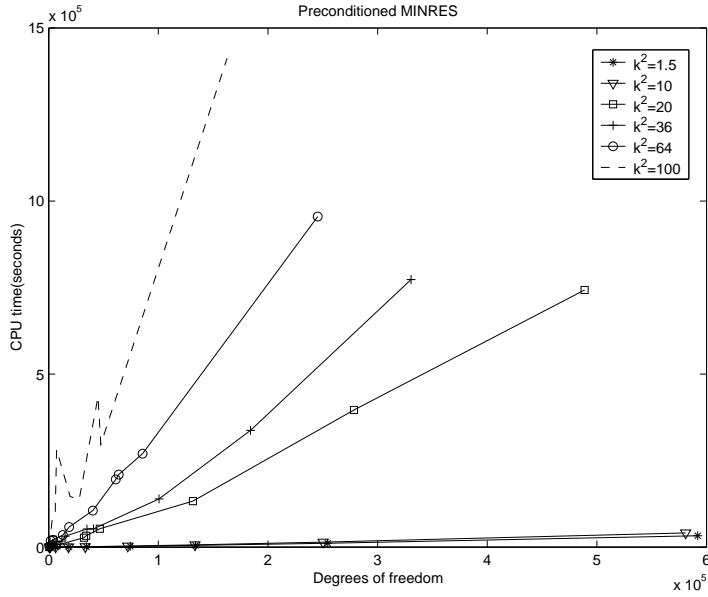


FIG. 5.9. CPU time for PMINRES iterations on adaptively refined meshes for  $\kappa^2 = 1.5, 10, 20, 36, 64, 100$  (Example 5.2).

TABLE 5.2

The Number of PMINRES iterations ( $N_{itrs}$ ) required to reduce the initial residual by a factor  $10^{-8}$  (Example 5.2) .

$\kappa^2 = 1$	Level	1	3	5	6	7	8	9
	DOFs	1322	18376	74655	137309	258991	599640	1022905
	$N_{itrs}$	36	32	32	32	31	31	31
$\kappa^2 = 1.5$	Level	1	3	5	6	7	8	9
	DOFs	604	6252	34471	74415	133960	254531	591946
	$N_{itrs}$	36	44	44	44	46	46	46
$\kappa^2 = 10$	Level	1	4	5	6	7	8	9
	DOFs	604	18040	33302	72094	133515	250203	580971
	$N_{itrs}$	44	56	58	56	58	58	58
$\kappa^2 = 20$	Level	1	4	5	6	7	8	9
	DOFs	604	32163	34225	46611	131532	278454	488868
	$N_{itrs}$	272	1091	1035	1068	879	854	833
$\kappa^2 = 36$	Level	1	3	5	7	8	9	10
	DOFs	604	3938	14956	40788	100672	184125	330495
	$N_{itrs}$	845	1917	3358	2166	2167	2231	2314
$\kappa^2 = 64$	Level	1	3	5	7	8	9	10
	DOFs	604	3603	16212	53104	55350	74246	212931
	$N_{itrs}$	2413	7012	6852	6757	6424	6547	7302
$\kappa^2 = 100$	Level	1	4	5	6	7	8	9
	DOFs	604	7224	19516	27888	45018	47534	162770
	$N_{itrs}$	2464	55223	15916	9437	17278	10479	15775

We remark that the frequency of the problem influences the total value of the a posteriori error estimate, but does not influence its reduction rate. These phenomena coincide with Theorem 3.3 and 3.4, where the frequency only influences the constants and the estimates in the theorem, but does not influence the convergence rate. Furthermore, the frequency make a strong impact on the performance of the preconditioned MINRES algorithm.

EXAMPLE 5.3. This experiment is to test the robustness of our method for cavity problems on non-Lipschitz domains. The scatter consists of two perfect tetrahedral conductors  $S_1$  and  $S_2$  with vertices

$$\begin{aligned} S_1 : & \quad (0, 0, 0), \quad (0.5, 0.5, -0.5), \quad (0, 0.5, -0.5), \quad (0, 0, -0.5) \quad \text{and} \\ S_2 : & \quad (0, 0, 0), \quad (-0.5, -0.5, 0.5), \quad (0, -0.5, 0.5), \quad (0, 0, 0.5). \end{aligned}$$

The computational domain is defined by  $\Omega = (-1, 1)^3 \setminus (S_1 \cup S_2)$  (see Fig. 5.10). We set  $\mu_r = \varepsilon_r = \lambda = \kappa = 1$  in (1.1) and (1.2) and define

$$\mathbf{f} := \mathbf{0}, \quad \mathbf{g} := \mathbf{curl} \mathbf{E}_i \times \nu - \mathbf{i} \kappa \mathbf{E}_{i,t},$$

where  $\mathbf{E}_i = (e^{iy}, 0, e^{iy})^T / \sqrt{2}$ . The non-dimensional wavelength here is  $\pi/\sqrt{3}$ .

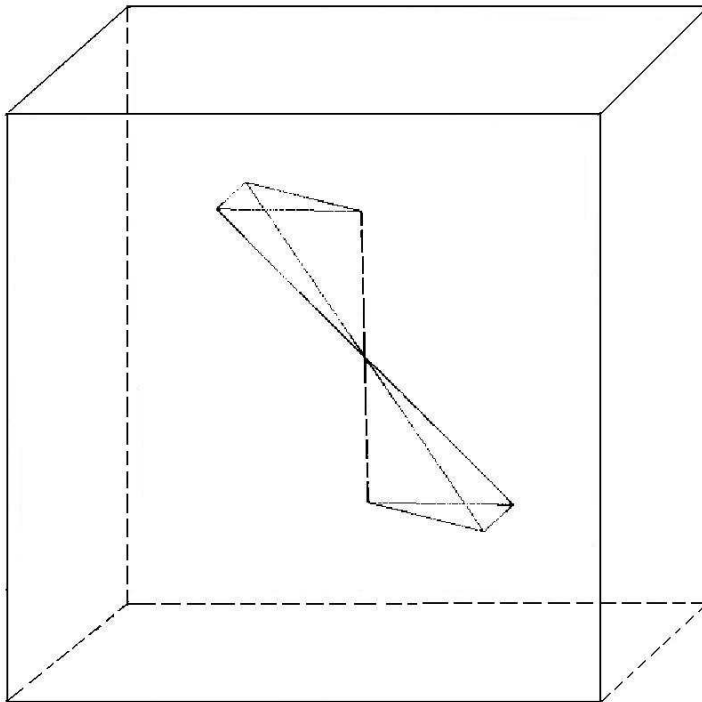


FIG. 5.10. Two tetrahedral conductors with a common vertex (Example 5.3).

Fig. 5.11 shows the  $\log \eta_k - \log N_k$  curves and indicate that the adaptive meshes and the associated numerical complexity are quasi-optimal and (5.2) is valid asymptotically. It also shows clearly the advantage of adaptive method compared with the uniform refinements.

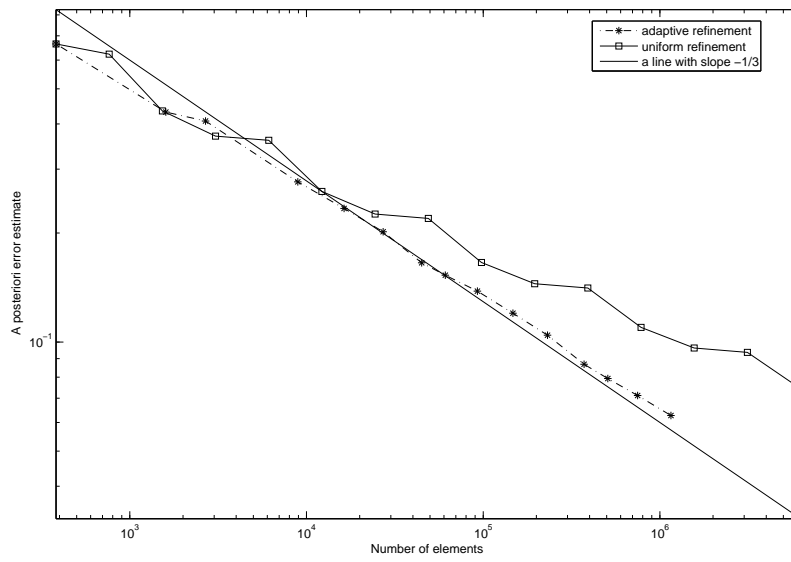


FIG. 5.11. *Quasi-optimality of the adaptive mesh refinements of the a posteriori error estimate (Example 5.3).*

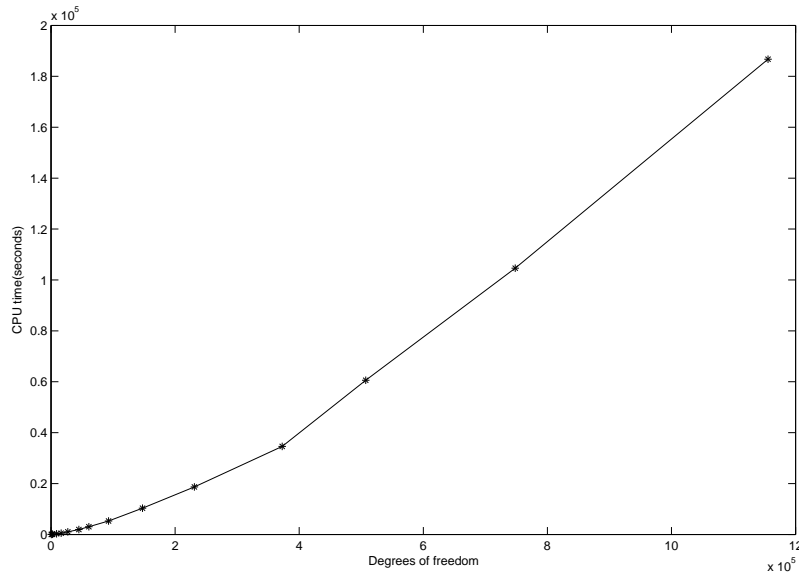


FIG. 5.12. *CPU time for PMINRES iterations on adaptively refined meshes (Example 5.3).*

Fig. 5.12 shows the CPU time versus the number of degrees of freedom on different adaptive meshes.

Table 5.3 shows the numbers of PMINRES iterations required to reduce the initial residual by a factor  $10^{-8}$  on different levels. We observe that it remains nearly fixed with the number of degrees of freedom varying from 2,102 to 1,394,075.

TABLE 5.3

*The Number of PMINRES iterations ( $N_{itrs}$ ) required to reduce the initial residual by a factor  $10^{-8}$  (Example 5.3) .*

Level	1	3	5	7	9	11	13	14
DOFs	2102	11134	33437	74735	179603	450971	903251	1394075
$N_{itrs}$	42	42	42	40	41	41	42	42

Fig. 5.13 shows an adaptive mesh of 1,856,117 elements after 15 adaptive iterations. We observe that the mesh is locally refined near the boundary of the scatterer.

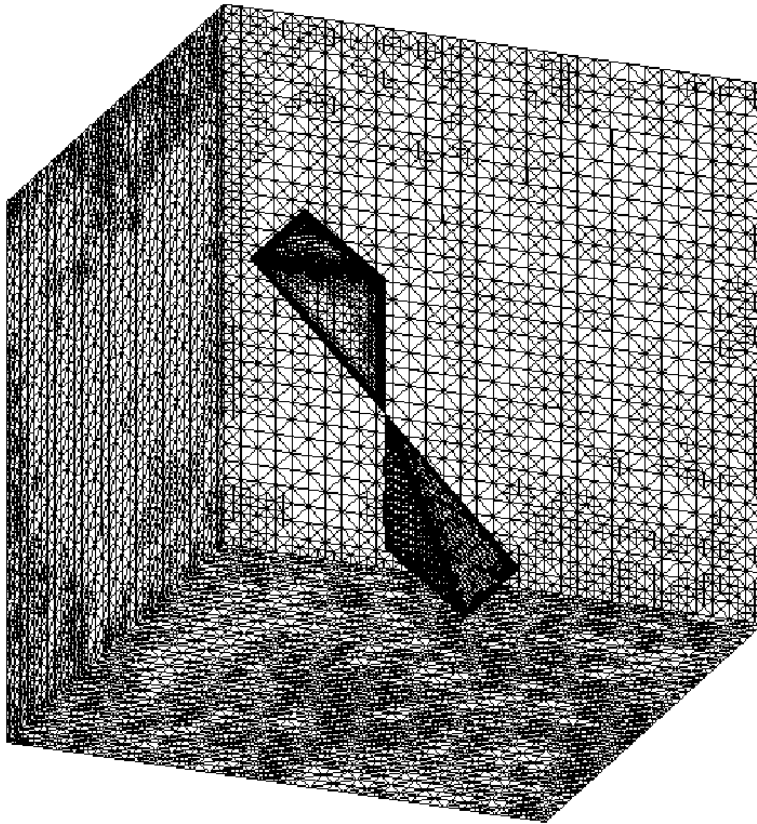


FIG. 5.13. *An adaptively refined mesh of 1856117 elements after 15 adaptive iterations (Example 5.3).*

## REFERENCES

- [1] D.N. ARNOLD, R.S. FALK, AND R. WINTHER, *Multigrid in  $H(\text{div})$  and  $H(\text{curl})$* , Numer. Math., 85(2000), pp. 197-217.
- [2] F. ASSOUS, P. CIARLET, JR., AND E. SONNENDRÜCHER, *Resolution of the Maxwell equations in a domain with reentrant corners*, Math. Model. Numer. Anal., 32 (1998), pp. 359-389.

- [3] I. BABUŠKA AND C. RHEINBOLDT, *Error estimates for adaptive finite element computations*, SIAM J. Numer. Anal. 15(1978), pp. 736-754.
- [4] I. Babuška and A. Aziz. *Survey Lectures on Mathematical Foundations of the Finite Element Method with Application to Partial Differential Equations*, ed. by A. Aziz, Academic Press, New York, 1973, 5-359.
- [5] A. BAYLISS, C.I. GOLDSTEIN, AND E. TURKEL, *On accuracy conditions for the numerical computation of waves*, J. Comput. Physics, 59 (1985), pp. 396-404.
- [6] R. BECK, R. HIPTMAIR, R.H.W. HOPPE, AND B. WOHLMUTH, *Residual based a posteriori estimators for eddy current computation*, M2AN Math. Modeling and Numer. Anal., 34 (2000), pp. 159-182.
- [7] R. BECK, P. DEUFLHARD, R. HIPTMAIR, R.H.W. HOPPE, AND B. WOHLMUTH, *Adaptive Multi-level Method for Edge Element Discretizations of Maxwell's Equations*, Surveys on Mathematics for Industry, 8(1998), pp. 271-312.
- [8] M.SH. BIRMAN AND M.Z. SOLOMYAK,  *$L^2$ -Theory of the Maxwell operator in arbitrary domains*, Uspekhi Mat. Nauk, 42 (1987), pp. 61-76 (in Russian); Russian Math. Surveys, 43 (1987), pp. 75-96 (in English).
- [9] M.SH. BIRMAN AND M.Z. SOLOMYAK, *On the main singularities of the electric component of the electro-magnetic field in regions with screens*, St. Petersburg Math. J., 5 (1994), pp. 125-139.
- [10] H. BLUM AND M. DOBROWOLSKI, *On finite element methods for elliptic equations on domains with corners*, Computing, 28(1982), pp. 53-63.
- [11] Z. CHEN AND S. DAI, *On the efficiency of adaptive finite element methods for elliptic problems with discontinuous coefficients*, SIAM J. Sci. Comput. 24(2002), pp. 443-462.
- [12] Z. CHEN AND S. DAI, *Adaptive Galerkin method with error control for a dynamical Ginzburg-Landau model in superconductivity*, SIAM J. Numer. Anal. 38(2001), pp. 1961-1985.
- [13] Z. CHEN, Q. DU, AND J. ZOU, *Finite element methods with matching and nonmatching meshes for Maxwell equations with discontinuous coefficients*, SIAM J. Numer. Anal., 37 (2000), No. 5, pp. 1542-1570.
- [14] Z. CHEN AND G.H. JI, *Sharp  $L^1$  a posteriori error analysis for nonlinear convection-diffusion problems*, Math. Comp., 75 (2006), 43-71.
- [15] Z. CHEN AND H. WU, *An adaptive finite element method with perfectly matched absorbing layers for the wave scattering by periodic structures*, SIAM J. Numer. Anal. 41(2003), pp. 799-826.
- [16] M. COSTABEL, *A remark on the regularity of solutions of Maxwell's equations on Lipschitz domains*, Math. Methods Appl. Sci., 12(1990), pp. 365-268.
- [17] M. COSTABEL AND M. DAUGE, *Singularities of electromagnetic fields in polyhedral domains*, Arch. Ration. Mech. Anal., 151(2000), pp. 221-276.
- [18] M. COSTABEL AND M. DAUGE, *Computation of resonance frequencies for Maxwell equations in non-smooth domains*, In: Topics on Computational Wave Propagation, M. Ainsworth et al eds., Springer-Verlag, Berlin, 2003, pp. 125-162.
- [19] A.B. DHIA, C. HAZARD, AND S. LOHRENGEL, *A singular field method for the solution of Maxwell's equations in polyhedral domains*, SIAM J. Appl. Math., 59(1999), pp. 2028-2044.
- [20] V. GIRAULT AND P. A. RAVIART, *Finite Element Methods for Navier-Stokes Equations*, Springer-Verlag, Berlin, 1986.
- [21] P. GRISVARD, *Elliptic Problems in Nonsmooth Domains*, Pitman, Boston-London-Melbourne, 1985.
- [22] J. GOPALAKRISHNAN, J.E. PASCIAK, AND L.F. DEMKOWICZ, *Analysis of a multigrid algorithm for time harmonic Maxwell equations*, SIAM J. Numer. Anal., 42 (2004), pp. 90-108.
- [23] R. HIPTMAIR, *Multigrid Method for Maxwell's Equations*, SIAM J. Numer. Anal., 36(1999), No. 1, pp. 204-225.
- [24] K. LI AND Y. MA, *Hilbert-space methods for Partial Differential Equations in Mathematical Physics (I)* (in Chinese), Xi'an Jiaotong University press, Xi'an, China, 1990.
- [25] W.F. MITCHELL, *Optimal multilevel iterative methods for adaptive grids*, SIAM J. Sci. Stat. Comput., 13 (1992), pp. 146-167.
- [26] P. MONK, *A posteriori error indicators for Maxwell's equations*, J. Comp. Appl. Math., 100(1998), pp. 173-190.
- [27] P. MONK, *Finite Element Methods for Maxwell's Equations*, Clarendon Press, Oxford, 2003.
- [28] P. MORIN, R.H. NOCHETTO, AND K.G. SIEBERT, *Data oscillations and convergence of adaptive FEM*, SIAM J. Numer. Anal., 38(2000), pp. 466-488.
- [29] J. NÉDÉLEC, *Mixed finite elements in  $R^3$* , Numer. Math., 35(1980), pp. 315-341.
- [30] J.E. PASCIAK AND J. ZHAO, *Overlapping Schwartz methods in  $H(\mathbf{curl})$  on polyhedral domains*,

- East West J. Numer. Math., 10(2002), pp. 221-234.
- [31] A. SCHMIDT AND K.G. SIEBERT, *ALBERT* – *An adaptive hierarchical finite element toolbox*, the new version ALBERTA is available online from <http://www.alberta-fem.de> .
  - [32] L.R. SCOTT AND Z. ZHANG, *Finite element interpolation of nonsmooth functions satisfying boundary conditions*, Math. Comp., 54 (1994), pp. 483-493.
  - [33] H. WU AND Z. CHEN, *Uniform convergence of multigrid V-cycle on adaptively refined finite element meshes for second order elliptic problems*, Research Report, No. 2003-07, Institute of Computational Mathematics, Chinese Academy of Sciences, 2003, available from [http://icmsec.cc.ac.cn/2003research\\_report.html](http://icmsec.cc.ac.cn/2003research_report.html) .